Geophys. J. R. astr. Soc. (1973) **35**, 243–264.

Calculation of Body Waves, for Caustics and Tunnelling in Core Phases†

Paul G. Richards

(Received 1973 January 15)

Summary

The known failure of classical ray theory at caustics has led to a reconsideration of displacement (in the frequency domain), expressed as an integral over ray parameter p. The integrand contains saddle-points on the real p-axis which correspond to rays for the associated physical problem, and it is shown here that direct computation of the complex integral is still straightforward, even when two saddle-points (rays) have coalesced to form a caustic. WKBJ theory is still usable for the vertical wave-functions, but one may avoid both the Taylor series expansion for the phase, and the steepest-descents approximation. Attention is first directed towards the *PKKP* caustic near 119°, to calculations of both amplitude and the phase slowness ($dT/d\Delta$) as a function of frequency, and to a criticism of some uses of plane wave reflection coefficients across the core–mantle boundary. It is then shown that short-period *P*-wave energy is efficiently tunnelled into and out of the Earth's core, from body waves having their turning point just above the core–mantle boundary. This provides an explanation for observations of multiply reflected core phases, *PmKP* with $m > 2$, which are found usually at distances beyond the cutoff one would expect from requiring real angles of incidence ($\leq 90°$) from mantle to core. To obtain body wave pulse shapes in the time domain, a method is described which appears to offer some strong advantages over Cagniard–de Hoop inversion.

Introduction

Advances in theoretical seismology have, in the last four or five years, made possible a much more complete use of the data contained in seismograms. Thus, the methods outlined by Helmberger (1968) and Gilbert & Helmberger (1972) are allowing the computation of theoretical seismograms in Earth models with fine layering down to scales of about 5 km in the upper mantle, and Helmberger & Wiggins (1971) have shown comparisons with seismic data along several profiles in North America. The time domain calculations of these authors are complemented by the frequency domain approach of Chapman & Phinney (1970, 1972), who have developed representations of the Fourier-transformed seismogram as an integral, typically over horizontal wavenumber, and have shown how direct numerical integration may be accomplished.

A consequence of these advances has been their demand for increasingly length and sophisticated computation—which is unfortunate (though often necessary), in that the expense and complexity of computations required by a full wave theory is a present barrier to routine applications of the theory by most seismologists.

† Lamont-Doherty Geological Observatory Contribution 2014.

This paper is concerned with the application of WKBJ approximations which can be made in the full wave theory—in particular, approximations which permit simple computations of short-period theoretical seismograms to be made, even in the vicinity of caustics. The computation involves modifying programs which are widely available: namely, programs giving travel time T, and distance Δ, for a ray with given ray parameter p in a specified Earth model, and programs giving plane-wave reflection and transmission coefficients. The principal modification involves allowing p to be complex.

Applications of the method of this paper are expected to arise in many different body wave problems: it is especially relevant to the evaluation of core phases. The method reduces trivially to the geometrical spreading formulae of Bullen (1963, Chapter VIII) and Julian & Anderson (1968), in cases where these are accurate, but it includes an evaluation of caustics, diffraction, and tunnelling, in cases where these are appropriate.

To illustrate basic procedures, the example of *PKKP* is considered in some detail at distances in the vicinity of a caustic near 241° (119° in the backward direction). This example shows that the use of plane-wave reflection and transmission coefficients, for short-period waves incident on the core–mantle boundary, may be suspect, and Airy functions are introduced to allow improvements in the basic method. They permit study of the excitation of core phases by mantle *P*-waves having turning points just above the core–mantle boundary. Such a tunnelling phenomenon is evaluated for *P*4*KP*, and is shown to be a remarkably efficient route of propagation. It appears (Engdahl 1968) frequently to have been observed.

Basic method

Wave propagation problems for point sources in layered media are often solved by Fourier (or Laplace) transformation of the time dependence, and also by transformation of the transverse spatial co-ordinate. (This latter is horizontal distance, for plane layering normal to a vertical axis, and is angular distance Δ, for spherically symmetric Earth models.)

The doubly-transformed wave-equation involves derivatives with respect to depth only, and yields an explicit formula for the doubly-transformed solution. After writing down the inverse transverse transform, over wavenumber, an integral representation is thus obtained for the forward time transform of the required solution. In the Cagniard–de Hoop methods, the integrand at this stage is manipulated into a form which permits its identification as the time-domain solution required. But, for frequency-domain calculations of the solution (see e.g. Chapman & Phinney 1972), the wavenumber integral is computed directly.

This paper uses the latter method, representing a Fourier-transformed seismogram at distance Δ from a point source as

$$s(\Delta, \omega) = \int_{\Gamma} f(\nu, \omega)\, Q_{\nu-1/2}^{(2)}(\cos\Delta)\, d\nu. \tag{1}$$

Here, ω is a radian frequency; Γ is a complex path which depends on the problem in hand; $f(\nu, \omega)$ is essentially the doubly-transformed solution; and $Q_{\nu-1/2}^{(2)}$ is that travelling-wave component in the Legendre function $P_{\nu-1/2}$ which moves away from the source. (The choice of $Q^{(2)}$, rather than $Q^{(1)}$, depends on our convention of the Fourer transform as $\int(\ )\,e^{+i\omega t}\,dt$. See Phinney & Alexander 1966; equation (19).) Equation (1) may take many different forms, depending on the Watson or Poisson transformation used to derive it, and on the particular rays (or routes of energy propagation) which it is intended to represent. Nussenzveig (1965) gives a thorough treatment in a spherical problem, and Scholte (1956) has discussed the representation of particular rays such as *PcP*, *PKP*, and diffraction by the Earth's core. Gilbert &

Helmberger (1972) have gone further in factorizing $f(\nu, \omega)$ into a product of (a) the source–receiver directivity function; and (b) the transmission and reflection coefficients appropriate to the ray path of interest (for the example of *PcP*, these include the core–mantle boundary reflection, transmission across mantle to crust, and, if required, a correction factor for measurements made on the free surface of the Earth). Included here also is the transmission phase for the total ray path, accumulated from the phases of the vertical wave functions, as they propagate across each layer of the model. Many authors (e.g. Friedman 1951; Seckler & Keller 1959) have shown that, for short periods, these vertical wave functions are accurately approximated by WKBJ theory.

In order to obtain the specific $f(\nu, \omega)$ in equation (1), for the numerical evaluation given below, the seismic source is taken to be an explosive point source at position $\mathbf{r} = \mathbf{r}_s$, with equivalent body force given by the gradient of potential $F\delta(\mathbf{r}-\mathbf{r}_s)\,H(t)$. ($H(t)$ here is the Heaviside unit step function and $\delta(\mathbf{r})$ is a three-dimensional Dirac delta function.) Were this source in a homogeneous elastic medium, with *P*-wave speed α_s and density ρ_s (suffix s refers throughout to evaluation at the source), it would give rise to a spherical *P*-wave wavefront, centred on the source. The displacement would have just a longitudinal component, u_l (say), directed away from the source. Near the wavefront, this component would be

$$u_l(\mathbf{r}, t) = \frac{-F\delta(t-R/\alpha_s)}{4\pi\rho_s\alpha_s^3 R} \tag{2}$$

in which R is the distance $|\mathbf{r}-\mathbf{r}_s|$, and $\delta(t)$ is a one-dimensional Dirac delta function. Head-waves from this source would have the shape of $H(t-R/\alpha_s)$, and the reduced displacement potential (see Werth & Herbst 1963) is $FH(t)/(4\pi\rho_s\alpha_s^3)$. If, as we assume, this source is placed in a spherically symmetric Earth, then the equation equivalent to (2) is the result obtained by classical ray theory:

$$u_l(\mathbf{r}, t) = -\frac{F\delta(t-T(\mathbf{r}, \mathbf{r}_s))}{4\pi(\rho\alpha)^{1/2}\rho_s^{1/2}\alpha_s^{5/2}R(\mathbf{r}, \mathbf{r}_s)}. \tag{3}$$

Here, ρ and α are evaluated at the receiver position $\mathbf{r}$; T is the *P*-wave travel-time to $\mathbf{r}$ from $\mathbf{r}_s$ taken along the ray connecting source and receiver; and $R(\mathbf{r}, \mathbf{r}_s)$ represents the geometrical spreading from source to receiver. This function is defined by requiring $R^2\,d\Omega$ to be the cross-sectional area, at $\mathbf{r}$, of a tube of rays which leaves $\mathbf{r}_s$ in a cone of solid angle $d\Omega$. The factor $(\rho\alpha)^{-1/2}$ in (3) arises from conservation of energy flux down ray tubes; the remaining $\rho_s^{-1/2}\alpha_s^{-5/2}$ are required for this source, so that equation (3) tends to the form (2) as $\mathbf{r} \to \mathbf{r}_s$ (noting then that $R(\mathbf{r}, \mathbf{r}_s) \to |\mathbf{r}-\mathbf{r}_s|$).

To appreciate the inaccuracy of (3), for many distances in realistic Earth models, and to improve the calculation of body wave amplitudes, a full wave theory is required. This theory is outlined below in a form which approximates, at two stages, the exact version often necessary for accurate studies of the upper mantle (although providing useful guidelines even in these cases).

The first approximation (Richards 1971a; 1973) permits the use of potentials, to discuss *P–SV* motion in a spherically symmetric (but radially varying) medium. It may be shown by construction that azimuthally independent scalar functions $\phi(\mathbf{r}, \omega)$, $\chi(\mathbf{r}, \omega)$ exist, such that displacement in the frequency domain is given by

$$\mathbf{u}(\mathbf{r}, \omega) = \frac{1}{\rho^{1/2}}\left[\operatorname{grad}\phi + \operatorname{curl}\left(0, 0, -\frac{\partial\chi}{\partial\Delta}\right)\right] + 0\left(\frac{\mathbf{u}}{\omega}\right). \tag{4}$$

The vector potential for S here is itself solenoidal, being curl $(r\chi, 0, 0)$, where vector components are written in spherical polar co-ordinates. Furthermore, the wave

equations satisfied by ϕ and χ are of second order, being

$$\nabla^2\phi+\frac{\omega^2}{\alpha^2(r)}\phi = K_s\delta(\mathbf{r}-\mathbf{r}_s)+0\left(\frac{|\mathbf{u}|}{\omega}\right)$$
$$\nabla^2\chi+\frac{\omega^2}{\beta^2(r)}\chi = 0\left(\frac{|\mathbf{u}|}{\omega^2}\right) \tag{5}$$

where the constant K_s, for our source normalization, is $F/(i\omega\rho_s{}^{1/2}\alpha_s{}^2)$, and β is the shear wave speed.

The lower-order terms, in the right-hand side of the last three equations, would vanish in a homogeneous medium. We shall neglect these terms, even in radially varying media, since they are down in magnitude from the remaining terms by a factor of ω^{-1}, or ω^{-2}, and we are interested in a theory which is accurate at high frequencies.

The solution of (5) in a homogeneous medium is merely

$$\phi = \frac{-K_s\,e^{ih_sR}}{4\pi R}, \quad \chi = 0$$

where $h_s = \omega/\alpha_s$. This has the well-known partial wave expansion in terms of spherical Hankel functions,

$$\phi = \frac{-K_s}{4\pi} ih_s \sum_{n=0}^{\infty} (n+\tfrac{1}{2})\, h_n{}^{(1)}(h_sr_>)[h_n{}^{(1)}(h_sr_<)+h_n{}^{(2)}(h_sr_<)]\, P_n(\cos\Delta)$$

where $r_>$ = the greater of (r, r_s), $r_<$ = the lesser of (r, r_s).

Friedman (1951) and Richards (1970, Appendix II) show that this last result may be generalized for a radially varying $\alpha(r)$, giving the particular integral of (5) as

$$\phi = L_s \sum_{n=0}^{\infty} (n+\tfrac{1}{2})\, g_n{}^{(1)}(r_>)[g_n{}^{(1)}(r_<)+g_n{}^{(2)}(r_<)]\, P_n(\cos\Delta) \tag{6}$$

where $L_s = -F/(4\pi\rho_s{}^{1/2}\alpha_s{}^3)$, and the $g_n{}^{(j)}$ are generalized vertical wave functions, outgoing (from the centre of the Earth) for $j = 1$, and ingoing for $j = 2$. The normalization of these wave functions is taken so that their WKBJ approximation (Morse & Feshbach 1953, p. 1101) is, in the region for which $\omega r > (n+\frac{1}{2})\,\alpha(r)$,

$$g_n^{(2)}{}^{(1)}(r) \approx \frac{e^{\mp i\pi/4}}{\omega r}\frac{(\alpha\,\alpha_s)^{1/2}}{[\ ]^{1/4}}\, e^{\pm i\omega\int_{r_n}^{r}([\ ]^{1/2}/\alpha)\,dr} \tag{7}$$

where

$$[\ ] \equiv \left[1-\frac{\alpha^2(n+\frac{1}{2})^2}{\omega^2r^2}\right]$$

and r_n is the radius at which the integrand vanishes. The right-hand side of (7) is made up from radially varying amplitude and phase factors (obtainable from the one-dimensional wave equation satisfied by the $g_n{}^{(j)}$), and a source dependent factor, chosen to make the $g_n{}^{(j)}$ exactly spherical Hankel functions in homogeneous media. There are analogies here to the way radial dependence in (3) was deduced from (2). Although the approximation (7) is to be used below in calculating the $g_n{}^{(j)}$, (7) has at this stage merely the role of normalizing the exact vertical wave functions.

It is often useful to split the Legendre function into its travelling wave components,

$$P_n = Q_n{}^{(1)}+Q_n{}^{(2)}$$

where (provided n is not near a negative integer, nor Δ near 0 or 180°)

$$Q_n^{(2)}{}^{(1)}(\cos\Delta) = \left(\frac{1}{2\pi n\sin\Delta}\right)^{1/2} e^{\mp i[(n+1/2)\Delta-\pi/4]}\left[1+0\left(\frac{1}{n}\right)\right]. \tag{8}$$

Conversely, it is often convenient to sum the vertical wave functions,

$$g_n^{(1)} + g_n^{(2)} = 2f_n, \quad \text{where } f_n \text{ is regular at } r = 0$$

and reduces to the spherical Bessel function j_n in homogeneous media.

Although partial wave expansions such as (6) are convergent series, the individual terms do not significantly decrease until n exceeds N, where

$$N \equiv \left. \frac{\omega r}{\alpha(r)} \right|_{r=r_<}.$$

The number N is about $4500 \div$ period (in seconds), so several thousand terms would have to be summed, if short-period body waves (with period about 1 or 2 s) were calculated directly via (6). Such numerical difficulty is effectively avoided by converting the summation over n into an integral (the Watson or Poisson transform), and then direct integration is simple to carry out, after a suitable contour is found in the (complex) order plane. Finding the suitable contour is not always easy (see Nussenzveig 1965, 1969a, b for an extensive analysis), since (6) is essentially a sum of four different types of waves. Each is of type $g_n^{(j)}(r_<)\, Q_n^{(k)}$, with $j = 1$ or 2, $k = 1$ or 2, and can be recognized in terms respectively of downward or upward departure from $r_<$ to $r_>$, and arrival towards or away from the source. But if the series (6) is separated into four series, one for each wave type, each series diverges. Fortunately, however, it appears that an integral representation of series (6) can always be found with the following two simplifying properties: (a) the integrand involves the conversion of just the expected one of the four terms in (6); and (b) the integrand contains no scalar factors not already explicitly displayed in the series (6).

To illustrate these simplifications, and to obtain two interesting representations of the particular integral (6), an Appendix is given below to describe the necessary manipulations in the complex order plate. Different representations are shown to arise, depending on whether or not a turning point is present, for the ray path between source and receiver.

It is well known that there is a relation between the order of a radial wave function, $g_n^{(j)}(r)(j = 1 \text{ or } 2)$, and the horizontal phase slowness of the wave solution $g_n^{(j)}(r)\, Q_n^{(2)}(\cos \Delta)\, e^{-i\omega t}$. In seconds/radian, the slowness is approximately $(n+\frac{1}{2})/\omega$. This result follows directly from equation (8), and hence tends to become more accurate as n increases. A much better physical discussion of the Appendix formulae can thus be given, if one shifts and scales the complex order plane by instead using the variable

$$p = (\text{order number} + \tfrac{1}{2})/\omega. \tag{9}$$

A further benefit of this transformation is the well-known interpretation of WKBJ approximations (7) in terms of ray properties: r_n is the turning point radius of the ray with ray parameter p; the $g_n^{(j)}$ grow exponentially with depth below r_n, but f_n decays exponentially; and the expression [ ] in (7) is merely $\cos^2 i$ where $i = i(r, p)$ is the angle between this ray at depth r and the local vertical. (We shall, however, find cause below to improve the approximation (7) in the vicinity of $r = r_n$.) Equation (7) then becomes

$$g^{(1)}_{\omega p - 1/2}{}^{(2)}(r) \approx \frac{e^{\mp i\pi/4}}{r} \left(\frac{\alpha \alpha_s}{\cos i} \right)^{1/2} \exp\left(\pm i\omega \int_{r_p}^{r} (\cos i/\alpha)\, dr \right) \tag{10}$$

in which, following Bullen (1963), r_p is the turning point radius of the ray with ray parameter p.

The Appendix formulae (A2) and (A3) can now be written as integrations in the complex ray parameter plane, and we have the following two cases:

Case A

Source below receiver, ray departing upwards (see Fig. 1(a)).

$$\phi(\mathbf{r}, \omega) = L_S \int_{\Gamma_1} \omega^2 p g_{\omega p-1/2}^{(1)}(r)\, g_{\omega p-1/2}^{(2)}(r_S)\, Q_{\omega p-1/2}^{(2)}(\cos\Delta)\, dp \qquad (11)$$

where Γ_1 is the path shown in Fig. 1(b).

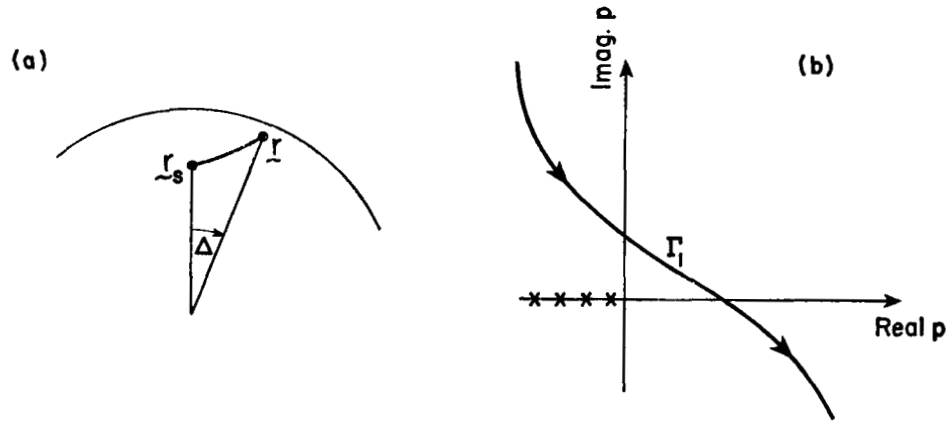

FIG. 1. (a) Parameters for a ray departing upwards from source to receiver. (b) Associated path Γ_1 for the response integral in the complex p plane. See equation (11).

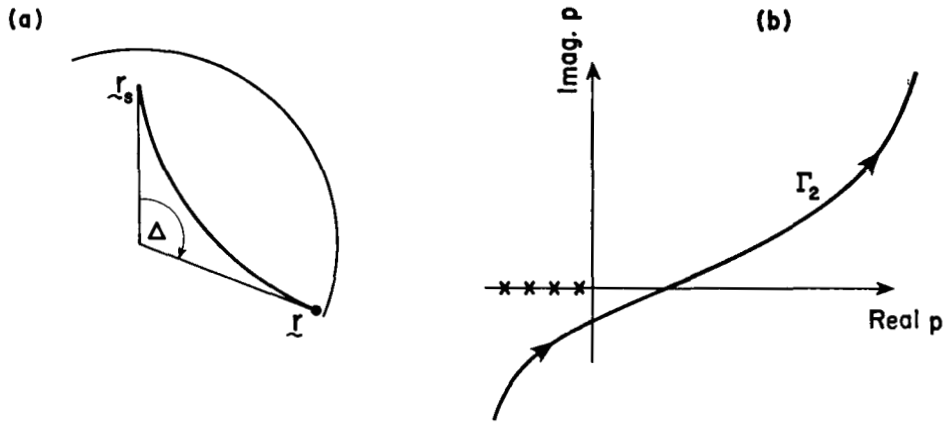

FIG. 2. (a) Parameters for a ray departing downwards from source to receiver. A turning point is present. (b) Associated integration path Γ_2. See equation (12).

Case B

Source below receiver, ray departing downwards (see Fig. 2(a)).

$$\phi(\mathbf{r}, \omega) = L_S \int_{\Gamma_2} \omega^2 p g_{\omega p-1/2}^{(1)}(r)\, g_{\omega p-1/2}^{(1)}(r_S)\, Q_{\omega p-1/2}^{(2)}(\cos\Delta)\, dp \qquad (12)$$

where Γ_2 is the path shown in Fig. 2(b).

The singularities of each of these integrands are merely poles on the negative real axis, and each of Γ_1 and Γ_2 may be deformed to cross any convenient point, or points, of the positive real p-axis. The effect of discontinuities in the Earth, such as the core–mantle boundary, is examined below, and equations (11) and (12) have a relatively

simple form because reflection and transmission coefficients are absent. The effect of multi-pathing between source and receiver is, however, included: the number of rays present must be odd, since implicit in the above definition of $g_n^{(j)}$ is the assumption that no low velocity zones are present. (The WKBJ expressions may be modified to permit weakening of this assumption.) It is well known that each ray path between $\mathbf{r}_s$ and $\mathbf{r}$ has a ray parameter which, at high frequencies, is near a saddle point of the integrands in (11) and (12)—and is exactly at the saddle point, if these integrands are replaced by the WKBJ expressions (8) and (10). Further, it can be shown that the orientation of saddles is such as to permit the path Γ to cross all of them by the route of steepest descents.

The uses made of these results have been either (i) to compute the vertical wave functions directly (by integration of the equations of motion), and then to integrate the results for Γ chosen near the steepest descents path (see e.g. Chapman & Phinney 1970), or (ii) to substitute from (8) and (10) into (11) or (12), and then to make a Taylor series expansion of the phase about each saddle point. If this series for the phase is approximated by only the first two non-zero terms, and if further the integral (11) or (12) is approximated by taking Γ separately over each saddle (and adding the results), then (as is shown below) one merely obtains geometrical spreading formulae of type (3). But a middle way between this trivial result and the numerical complexity of (i) is available, and involves the numerical integration of formulae such as (11) and (12), but using the WKBJ approximations for the integrand. This is the second stage of approximation, referred to prior to equation (4). It permits rapid computation of body wave amplitudes, even in cases of multi-pathing, and is particularly useful for distances near caustics. The method is computationally very simple, as can be seen on applying it to, for example, the radial component of displacement in Case B (with turning point: see Fig. 2). Then, for a receiver at distance Δ_0 from the source, we have

$$u_r(r, \Delta_0, \omega) = \rho^{-1/2}\, \partial\phi/\partial r.$$

The stage two approximation, obtained from (12), (8) and (10) after differentiating the approximation for $g_{\nu-1/2}^{(1)}(r)$ and retaining terms of highest order in frequency, is

$$u_r(r, \Delta_0, \omega) = e^{-i\pi/4} \frac{\alpha_s L_s}{r r_s} \left(\frac{\omega \alpha_s}{2\pi\rho\alpha \sin \Delta_0}\right)^{1/2} \int_{\Gamma_s} \left(\frac{p \cos i}{\cos i_s}\right)^{1/2} e^{i\omega J(r,\, p)}\, dp \qquad (13)$$

where

$$\cos i = \left(1 - \frac{\alpha^2 p^2}{r^2}\right)^{1/2}, \quad \cos i_s = \left(1 - \frac{\alpha_s^2 p^2}{r_s^2}\right)^{1/2}$$

and the phase delay integral is

$$J(r, p) = \int_{r_p}^{r_s} \left(\frac{\cos i}{\alpha}\right) dr + \int_{r_p}^{r} \left(\frac{\cos i}{\alpha}\right) dr + p\Delta_0.$$

Notes on equation (13)

(i) If the fourth-order equations for *P–SV* motion in spherical geometry are solved by the generalized WKBJ method of Coddington & Levinson (1955, pp. 174–177), then (13) can be obtained without the device of introducing approximate potentials (equation (4)). See Chapman (1973) for discussion of this method.

(ii) The horizontal displacement is given by (13), but with integrand modified by the factor $p\alpha/(r \cos i)$.

(iii) The turning-point radius r_p is complex if p is complex. It is a solution of the equation $p\alpha(r) = r$, and thus the velocity profile must be analytically continued from its values at real depths. This can be achieved for ray parameters with small imaginary

part, by Taylor series expansion of the velocity profile about a real radius. It is also simple to achieve for velocity profiles given by some specific analytic expression, such as the Mohorovičić law, $\alpha(r) = ar^b$. If a low velocity zone is present, then r_p is no longer a single valued function of p. Knowledge of the turning point is not needed for ray paths of the type shown in Fig. 1, since there the phase arises from the phase of $g_{\nu-1/2}^{(1)}(r)\, g_{\nu-1/2}^{(2)}(r_s)$, and involves merely an integral from r_s to r.

(iv) As pointed out by Bullen (1963, p. 112) and Gilbert & Helmberger (1972), the phase delay integral in (13) is related to the travel-time and distance integrals, and in fact one finds in all cases that

$$J(r,p) = T(r,p) - p\Delta(r,p) + p\Delta_0 \tag{14}$$

where T and Δ are the time and distance at which the ray with ray parameter p arrives, at radius r, from source r_s. Since $\partial T/\partial p = p\ \partial\Delta/\partial p$, it follows that the integrand for u_r has saddle points at values of p such that $\Delta(r,p) = \Delta_0$, i.e. at just the ray parameters for which there is a ray between source and receiver. Near such a saddle point p_0 (say), Taylor series expansion gives

$$J(r,p) = T(r,p_0) + \tfrac{1}{2}(p-p_0)^2(-\partial\Delta/\partial p).$$

If there is just one real ray between $\mathbf{r}$ and $\mathbf{r}_s$, then (from the curvature of the travel-time curve) $\partial\Delta/\partial p$ is negative, and the saddle is oriented favourably for Γ_2 to be taken as the path of steepest descent, leading to the approximation of (13) by

$$u_r(r, \Delta_0, \omega) = \alpha_s L_s \left(\frac{\alpha_s}{\rho\alpha}\right)^{1/2} \frac{e^{i\omega T}}{rr_s} \left[\frac{\cos i_s \sin \Delta_0}{p_0 \cos i} \left(\frac{-\partial\Delta}{\partial p}\right)\right]^{-1/2}.$$

Using the formula for L_s, and the geometrical spreading relation

$$\alpha_s R(\mathbf{r}, \mathbf{r}_s) = rr_s[\cos i \cos i_s \sin \Delta_0 |\, \partial\Delta/\partial p\, |/p_0]^{1/2}$$

(see Richards 1971b, p. 463), we have

$$u_r(r, \Delta_0, \omega) = \frac{-F\, e^{i\omega T} \cos i}{4\pi(\rho\alpha)^{1/2}\, \rho_s^{1/2} \alpha_s^{5/2} R(\mathbf{r}, \mathbf{r}_s)} \tag{15}$$

which is in complete agreement with equation (3), after resolving the longitudinal motion in the radial direction, and Fourier inversion.

A more complex configuration is shown in Fig. 3(a), where for the distance Δ_0 there are five ray parameters which solve the equation $\Delta(r,p) = \Delta_0$. The second

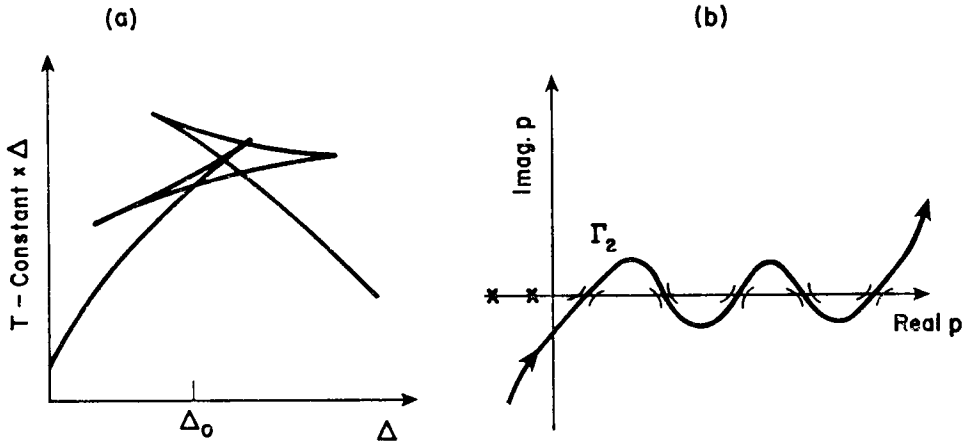

FIG. 3. (a) A reduced travel-time curve, with two over-lapping triplications. (b) Integration path in the complex ray parameter plane, crossing five saddles, each at a value of p satisfying $\Delta(r,p) = \Delta_0$.

derivative of the phase integral, $-\omega\ \partial\Delta/\partial p$, is alternately positive and negative, giving saddles with the orientation shown in Fig. 3(b). Γ_2 may be deformed to cross each saddle by the steepest descents path, to give approximations of the type (15) for the first, third and fifth saddles. For the second and fourth, the approximation is of type (15) times $(-i)$. Our analysis has been for the case of positive frequencies. The negative frequency solution can be found from the requirement that $\mathbf{u}(\mathbf{r}, t)$ be real, implying that the Fourier transform has a real part which is even in ω, and an imaginary part which is odd. Inverting to the time domain, arrivals corresponding to the first, third and fifth saddles thus behave like $-\delta(t-T)$, but for the second and fourth the time dependence is the allied function, $[\pi(t-T)]^{-1}$ obtained by Hilbert transformation.

These approximate evaluations of integral (13) are accurate only if the saddles in Fig. 3(b) are sufficiently separated. If the distance Δ_0 is near a caustic, then two adjacent saddles may be sufficiently close for their contributions to interfere. Although this effect can be analysed with the use of uniformly asymptotic approximations to the integrand (Chester *et al.* 1957), it may numerically be simpler to compute the integral (13) directly, using (14) for the phase. This procedure is followed below.

(v) The final point to note in equation (13) is that a smoothly varying velocity profile has been assumed. If discontinuities are to be allowed for, such as the Earth's free surface, then the associated reflection and transmission coefficients must be introduced. The principal techniques involved are well known (Scholte 1956) for simple Earth models consisting of a few homogeneous shells, since in these the vertical wave functions at any depth are made up from spherical Hankel functions, which have been widely studied. It is found in such models that the wave path of interest (for example, *SKJKP*) can be analysed by isolating its partial wave series in the Debye ray expansion for the total response. A Watson transform can still be used, but now any path deformation in the complex ν-plane must take account of poles in the reflection/transmission coefficients for the ray path of interest. These poles are located by studying properties of the WKBJ approximation to spherical Hankel functions (Scholte 1956),

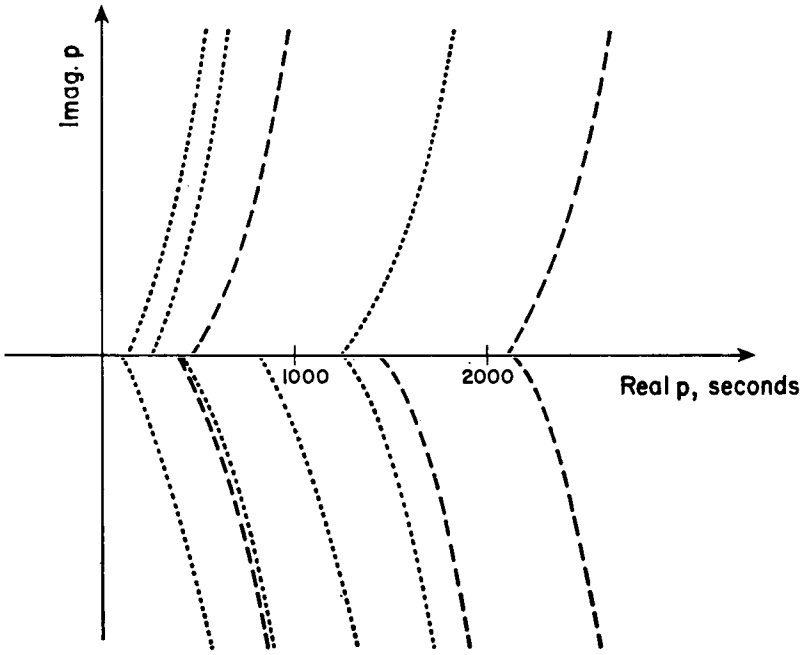

FIG. 4. Approximate location of diffraction poles, for the Earth model described in Table 1. Short dashes are used for *P* wave poles, long dashes for *S*.

and so in more realistic Earth models, with radial variation of elastic properties between depths of discontinuity, we may still expect to locate relevant poles by using WKBJ formulae (7) for the generalized vertical wave functions $g_{\nu-1/2}^{(J)}$. If the wave path under discussion has some interaction with the Earth's free surface, and with discontinuities between the crust and mantle, mantle and core, and outer core and inner core, then the associated poles may be expected to be near the schematic dashed lines shown, in the complex ray parameter plane, in Fig. 4.

Table 1

Body wave velocities in a Jeffreys–Bullen Earth model, with parameters also for a homogeneous crust and solid inner core. The last two columns give grazing-ray ray parameters for each interface.

Discontinuity	Radius r (km)	α (kms^{-1})	β (kms^{-1})	r/α (s)	r/β (s)
Free surface	6371	5	3	1274	2124
Crust	6338	5	3	1268	2113
Mantle	6338	7·75	4·353	818	1456
Mantle	3473	13·64	7·302	255	476
Outer core	3473	8·1	0	429	—
Outer core	1250	9·4	0	133	—
Inner core	1250	11·16	3	112	417

This diagram is for an Earth model with the discontinuities described in Table 1. Poles are located on lines starting near (but not on) the real p-axis, starting near real values each of which corresponds to a ray (either P or S) bottoming at one side of a discontinuity. The poles string upwards or downwards according to whether the grazing ray is just above or just below the interface. The complex p-plane contains also: poles in the left half plane which are the reflection in the origin of those shown in Fig. 4: poles corresponding to Stoneley or Rayleigh waves for each interface; and poles arising from the Watson transformation itself.

The rigorous analysis of path deformations, needed to change the Watson path (Fig. A1(a)) into paths such as Γ_1 or Γ_2 (Figs 1(b) and 2(b)) presents a formidable prospect for realistic Earth models. However, such solutions need rarely be achieved, or even attempted, since sufficient guidance appears to be obtained from insight into properties of the complex ray parameter plane, plus occasional rigour for canonical problems.

Briefly reviewing the major properties: the poles shown in Fig. 4 are associated with diffracted waves, the best seismological example being P diffracted along the bottom of the mantle (Phinney & Alexander 1966), and leading to energy leaking into the core shadow. Most such types of diffracted waves in fact have negligible contribution to seismograms: for example, S waves diffracted around the surface of the inner core, with a ray parameter of about 420 s. (Such waves could be excited only by tunnelling of P-wave energy through most of the outer liquid core.) A further simplifying feature is that Watson transforms are taken of partial wave series which in general are odd in ν, immediately permitting the Watson path to be taken just above (or just below) the entire real ν-axis. Each WKBJ approximation, a function of p and a radius r_j (say), is accurate for all positions along this integration path, except for the vicinity of two values p_j and $-p_j$, where $p_j = r_j/\alpha(r_j)$ (or $p_j = r_j/\beta(r_j)$, for S-wave functions). Since the radii at which vertical wave functions are needed include those at which boundary conditions enter the problem, the r_j are just those radii at which discontinuities are present in elastic parameters. For p near these p_j (listed for one model in the last two columns of Table 1), the wave functions are proportional to Airy functions with small (of order 1) argument. Linear combinations of these and their derivatives, appearing in the denominator of reflection/transmission coefficients, have zeros which generate the poles of importance in Fig. 4. Perhaps the major

simplifying feature of WKBJ methods is that the reflection/transmission coefficients turn out to be those for plane waves, incident on the boundary between two homogeneous half-spaces. The cases of near-critical incidence arise in just the cases that p is near some p_j, and the familiar branch cuts of planar problems have their analogue in the lines of poles shown in Fig. 4.

Gilbert & Helmberger (1972) have used several of the basic methods described in this section. Their work required path deformations which permit integrals such as (13) to be interpreted as a forward time transform, taking the WKBJ phase delay (i.e. $J(r, p)$) itself as the independent variable of integration. Their method, though often powerful, was not directly applicable for ray paths with turning points; nor was its use of wave reflection/transmission coefficients modified for near-critical incidence on spherical discontinuities. These drawbacks are absent from the present approach, which is illustrated by calculations for particular core phases.

Applications

We first examine *PKKP* at distances near 241°, which include a caustic. The radial displacement is given by (13), after inclusion of integrand factors giving coefficients for transmission into the core, reflection from below the mantle, transmission back into the mantle, and an extra phase shift $(-\pi/2)$ due to an extra turning point. The choice of dependent variable (potential, or displacement), used to obtain these coefficients, is unimportant, since only their product is needed. If receiver and source radii are equal, we have

$$u_r(r_s, \Delta_0, \omega) = \frac{F\, e^{i\pi/4}}{4\pi\rho_s\alpha_s{}^2 r_s{}^2}\left(\frac{\omega}{2\pi \sin\Delta_0}\right)^{1/2} \int_\Gamma p^{1/2} T_{PK} R_{KK} T_{KP}\, e^{i\omega J}\, dp \qquad (16)$$

with coefficients

$$T_{PK} = 2\rho_m\alpha_c \cos i_m \cos 2j_m/D$$

$$R_{KK} = [D - 2\rho_c \cos i_m]/D$$

$$T_{KP} = 2\rho_c\alpha_m \cos i_c \cos 2j_m/D$$

and

$$D = \rho_c\alpha_c \cos i_m + \rho_m[\alpha_m \cos^2 2j_m + 4s^2\beta_m{}^3 \cos i_m \cos j_m] \cos i_c$$

where suffix m refers to the bottom of the mantle, c to the top of the core, and the dependence on ray parameter (required for evaluation of (16)) is via

$$\cos i_x = (1 - p^2\alpha_x{}^2/r^2)^{1/2} \quad (x = \mathrm{m}, \mathrm{c}) \quad s = p/r$$

$$\cos j_m = (1 - p^2\beta_m{}^2/r^2)^{1/2} \quad \cos 2j_m = 1 - 2p^2\beta_m{}^2/r^2 \quad r = r_m.$$

The phase factor may be obtained from equation (14), using standard methods for calculating travel time and distance for a ray with given take-off angle, or ray parameter. The method used here is given by Julian & Anderson (1968, their Appendix), assuming the law $\alpha = ar^b$ in each layer of the Earth model given in Table 2.

To evaluate the integral in (16) for displacement, it remains to determine the path Γ. For the model of Table 2, a caustic is present in *PKKP* (surface focus) at $\Delta_c = 240{\cdot}8°$, with ray parameter $p_c = 227$ s. For $\Delta_0 > \Delta_c$ there are two real ray paths, with saddles at p', p'' as in Fig. 5(a). This figure also shows a steepest descents path Γ, crossing each saddle. For $\Delta_0 < \Delta_c$, the equation $\Delta(r, p) = \Delta_0$ has two complex conjugate roots, giving saddles as in Fig. 5(b). In this case, the steepest descents choice of Γ is taken across one saddle only. (The steepest descents crossing of the other saddle would be in a direction through p'', parallel to the imaginary p-axis.) This choice of path begins and ends in the same regions of the p-plane as in Fig. 5(a), and is a path for which the integrand contributions to u_r are effectively concentrated on a short length. Integrand singularities nearest $p = p_c$ occur near $p_j = 254{\cdot}6$ s,

Table 2

An Earth model (α, β, ρ), *specified at* 18 *radii. Values are taken from Jeffreys* (1962, *pages* 122 *and* 161), *with a solid inner core and homogeneous crust.*

Radius r (km)	α (kms^{-1})	r/α (s)	β (kms^{-1})	ρ (gcm^{-3})
125	11·305	11·06	3	17·2
500	11·28	44·33	3	17·0
1000	11·21	89·21	3	16·8
1250$^-$	11·16	112·01	3	16·8
1250$^+$	9·40	132·98		14·2
1389·2	10·44	133·07		11·54
2778·4	9·03	307·69		10·34
3473$^-$	8·10	428·77		9·43
3473$^+$	13·64	254·62	7·302	5·68
3802·8	13·46	282·53	7·199	5·52
4436·6	12·71	349·06	6·893	5·20
5323·92	11·50	462·95	6·395	4·71
5830·96	9·91	588·39	5·463	3·99
5894·34	9·50	620·46	5·227	3·82
5957·72	8·97	664·18	4·962	3·64
6338$^-$	7·75	817·81	4·353	3·32
6338$^+$	6	1056·33	3·5	2·7
6371	6	1061·83	3·5	2·7

associated with rays in the mantle incident at near grazing angles ($i_m \sim 90°$) on the core. These singularities, shown in Fig. 5(d), are well away from the paths Γ of either Fig. 5(a) or (b), and numerical evaluation of (16) can be achieved for all Δ_0 near Δ_c with the path Γ of Fig. 5(c).

The positions and orientations of saddles in Fig. 5(a) and (b) are similar to those

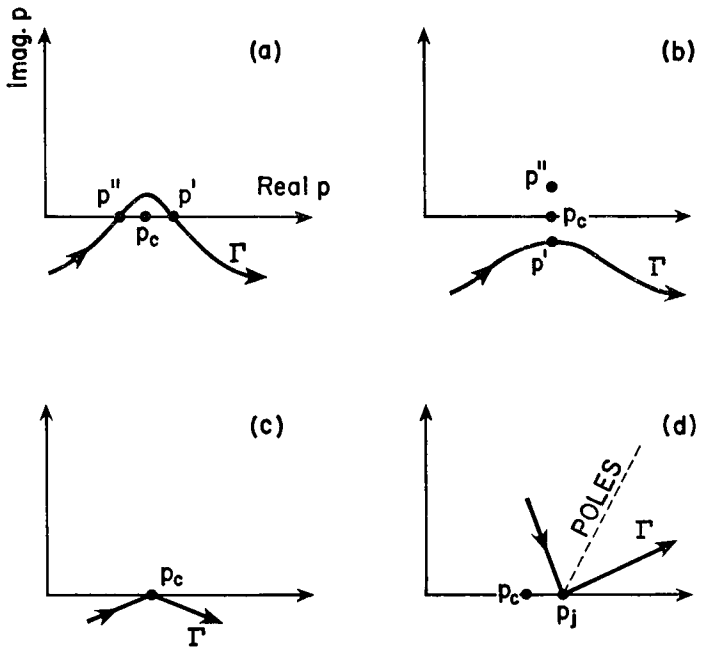

FIG. 5. Disposition of saddle points p' and p'', singularities, and resulting paths Γ for the cases: (a) *PKKP* at distances $\Delta_0 > \Delta_c$; (b) *PKKP* at $\Delta_0 < \Delta_c$; (c) choice of Γ as two line segments, appropriate for numerical work for all distances Δ_0 near Δ_c; and (d) the path for *P*+*PcP* at distances near the shadow boundary of the Earth's core.

of an Airy function with negative (Fig. 5(a)) or positive (Fig. 5(b)) argument. Jeffreys (1939) has attempted to use Airy's diffraction theory for the caustic in *PKP*, but such a geometrical method does not account correctly for the curvature of rays in an inhomogeneous medium. Such curvature is described in our problem by the positive quantity

$$B = \frac{\partial^2 \Delta}{\partial p^2}\bigg|_{p=p_c}$$

the model of Table 2 giving $B = 0{\cdot}000212\ \mathrm{s}^{-2}$. Note then that the phase delay $J = J(\Delta_0, p)$ can be expanded about (Δ_c, p_c) in the form

$$J(\Delta_0, p) = T_c + (\Delta_0 - \Delta_c)\, p - B(p - p_c)^3/6 \tag{17}$$

(correct to third order in small quantities $\Delta_0 - \Delta_c$, $p - p_c$) where

$$T_c = T(p_c) = J(\Delta_c, p_c) = \text{travel time to distance } \Delta_c.$$

To approximate displacement near a caustic, we may then substitute (17) in (16), evaluating all but the phase at $p = p_c$, and obtain

$$u_r(r_s, \Delta_0, \omega) = \frac{F\, e^{i\pi/4}}{4\pi \rho_s \alpha_s^2 r_s^2} \left(\frac{\omega}{2\pi \sin \Delta_0}\right)^{1/2} p^{1/2} T_{PK} R_{KK} T_{KP} \bigg|_{p=p_c} I. \tag{18}$$

Here,

$$I = \int_\Gamma \exp i\omega [T_c + (\Delta_0 - \Delta_c)\, p - B(p - p_c)^3/6]\, dp$$

$$= e^{i\omega [T_c + (\Delta_0 - \Delta_c)\, p_c]}\, 2 \int_0^\infty \cos \omega [(\Delta_c - \Delta_0)\, \mu + B\mu^3/6]\, d\mu.$$

This last integral is an Airy function (Abramowitz & Stegun 1964, equation 10.4.32), and

$$I = 2\pi\, e^{i\omega [T_c + (\Delta_0 - \Delta_c)\, p_c]}\, (\tfrac{1}{2}\omega B)^{-1/3}\, Ai[(\tfrac{1}{2}\omega B)^{-1/3}\, \omega(\Delta_c - \Delta_0)]. \tag{19}$$

Before turning to the numerical evaluation of (16), (18) and (19), it is of interest to note that the ray configuration of *PKKP* occurs also for light rays refracted and reflected by a sphere of water in air. Enhanced amplitudes near the caustic of once internally-reflected rays (*PKKP*) are responsible for the primary rainbow. Secondary and tertiary rainbows are occasionally observed in nature, at directions the seismologist would associate with caustics in *P3KP*, *P4KP*. Nussenzveig (1969b) discusses the scattering amplitude for these cases, and his Fig. 8 gives an integration path of the type needed in our present problem.

The numerical evaluation of equations (16) and (14) for displacement near the caustic in *PKKP* is shown in Fig. 6, which displays both slowness and logarithmic amplitude of the vertical component. Crustal reverberations here are ignored, being obtainable from Haskell's (1962) method, if needed. The slowness (reciprocal of horizontal phase velocity) is found by differentiation of the phase of u_r with respect to Δ_0, and division by ω. The calculations are carried out for two different periods, $\frac{1}{2}$ s and 2 s. For the longer period, the approximate method of equations (18) and (19) is also displayed over distances Δ_0 such that the argument of the Airy function in (19) has magnitude less than one. These results may be compared with the predictions of ray theory, which in Fig. 6 are shown as the ray parameter curve $p = p(\Delta_0)$ and as the amplitudes obtained (from geometrical spreading and plane wave reflections and transmissions) for each branch on the lit side of the caustic.

A principal feature of Fig. 6 is the way in which, at finite frequencies, both the slowness and the amplitude of the arriving displacement wave are close to just one of the ray theory branches. One might have expected stronger interference between the two branches, but this does not happen because the reflection coefficient R_{KK}

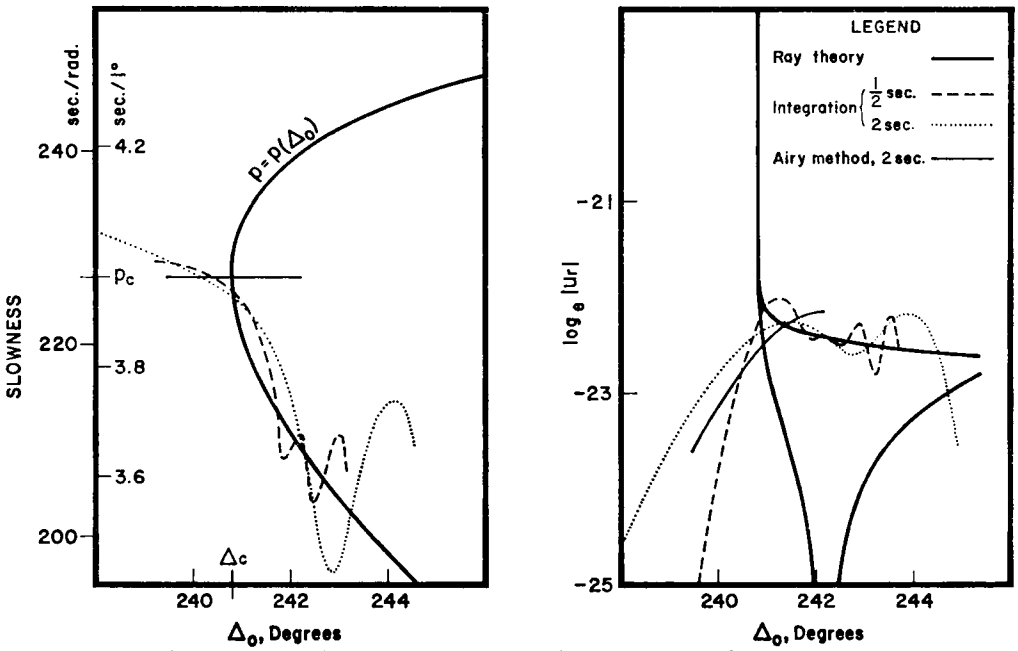

FIG. 6. Slowness and amplitudes for *PKKP* in the Earth model of Table 2. A caustic is present at $\Delta_0 = \Delta_c = 240{\cdot}8°$, and calculations are shown on the basis of ray theory; numerical integration of equation (17) for two different periods; and Airy diffraction, allowing for ray curvature (equations (19) and (20)). One branch of the ray theory amplitudes has a zero at $\Delta_0 = 242\frac{1}{4}°$ due to a zero in reflection coefficient R_{KK} at ray parameter value $p = 240$ s.

turns out to be much smaller for values of p on the second branch ($p > p_c$), going through a zero near $p = 240$ s. Despite such variations in a factor of the integrand in (16), the Airy method is quite good for amplitudes near Δ_0. However, it appears poor for slowness. Amplitudes given by (16) are down by a factor of 10, for waves of 2-s period, at about 3° into the shadow side of the caustic, and for $\frac{1}{2}$-s period this decay is reached at about 1°.

The apparent success of the numerical integration method for calculating *PKKP* suggests its use to investigate other core phases. Engdahl (1968) has reported observations of *PmKP* up to $m = 5$, reproducing a record of *P4KP*, and Bolt & Qamar (1972) have obtained records of P7*KP*. But the caustics for *P4KP* and *P7KP* occur, in the crude Earth model of Table 2, for $p_c = 246{\cdot}5$ s and 251·6 s respectively (at distances $\Delta_c = 415{\cdot}4°$ and $668{\cdot}0°$). Such slowness values are close to $p_f = 254{\cdot}6$ s, the value for mantle *P* waves at grazing incidence on the core. The difficulty is thus raised that solution integrands, of the type in (16), have their main contribution at ray parameter values near a system of singularities of the type shown in Fig. 4. The problem is not that any extra residues are picked up by the integration, or that the integrand is ill-behaved: it is simply that the WKBJ expression (9) is inaccurate for values of p ($= (n+\frac{1}{2})/\omega$) near the slowness value which makes the radial argument a turning point. The physical limitation imposed by this breakdown is that plane wave reflection/transmission coefficients are inadequate to investigate grazing incidence of a wave upon a spherical boundary. To investigate the extent of the inaccuracy, and to improve on (9) where necessary, consider the one-dimensional wave equation satisfied by $g_n^{(2)}(r)$:

$$\frac{d^2}{dr^2}(rW) + \left[\frac{\omega^2}{\alpha^2(r)} - \frac{n(n+1)}{r^2}\right](rW) = 0 \qquad (20)$$

where W is a vertical wave function (a spherical Bessel function, if α were constant).

For r near the turning point radius, the solution of (20) is given by Airy functions, using a method going back to Rayleigh (1912). But we wish to investigate solutions $W = W(r, n)$ with n varying and r fixed. Richards (1970) has shown in this case that the normalization implicit in (7) leads to

$$g_{\omega p-1/2}^{(1)(2)}(r) = c_1\omega^{-5/6}\,e^{\mp i\pi/3}[Ai(z\,e^{\pm 2i\pi/3})+0(\omega^{-2/3})] \tag{21}$$

where the quantity z is linearly related to p via $z = c_2\omega^{2/3}[p-r/\alpha(r)]$, and the real frequency-independent constants c_1, c_2 are $c_1 = (2/r)^{5/6}(\pi\alpha_s)^{1/2}\alpha^{1/3}(1-b)^{-1/6}$, with $b = (r/\alpha)(d\alpha/dr)$; $c_2 = (2\alpha/r)^{1/3}(1-b)^{-2/3}$.

Formulae (21) enter the analysis of core phases via the $\cos i_m$ of (16), since this expression arose in the plane wave theory from the ratio of the radial derivative of a mantle P wave function to the function itself: different signs arise for this ratio using upgoing or downgoing plane waves, and these cases must be distinguished if (21) are used, since the two directions then give ratios which are not so simply related. The resulting coefficients across the core–mantle boundary thus become

$$T_{PK} = \rho_m\alpha_c[C^{(1)}+C^{(2)}]\cos 2j_m/D$$

$$R_{KK} = [D-2\rho_cC^{(1)}]/D$$

$$T_{KP} = 2\rho_c\alpha_m\cos i_c\cos 2j_m/D,$$

where

$$D = \rho_c\alpha_cC^{(1)}+\rho_m[\alpha_m\cos^2 2j_m+4s^2\beta_m{}^2C^{(1)}\cos j_m]\cos i_c,$$

and

$$C^{(1)}_{(2)} = \pm i\,e^{\pm 2i\pi/3}\left(\frac{2\alpha_m(1-b_m)}{\omega r_m}\right)^{1/3}\frac{Ai'(z_m\,e^{\pm 2i\pi/3})}{Ai(z_m\,e^{\pm 2i/3})}, \tag{22}$$

suffix m indicating evaluation at the base of the mantle, and $Ai'(\xi)$ being $(d/d\xi)\,Ai(\xi)$.

As p decreases below the core-grazing value (r_m/α_m), $C^{(1)}$ and $C^{(2)}$ both become (approximately) $\cos i_m$, and the wave coefficients in (22) match on to those of (16). But as p increases above r_m/α_m, one finds

$$C^{(1)} \sim i(p^2\alpha_m{}^2/r_m{}^2-1)^{1/2} \sim -C^{(2)}, \quad \text{and} \quad T_{PK}\to 0.$$

For intermediate values of p, formulae (22) quantify a tunnelling effect: P-waves which have turning points just above the core can leak energy down into the core. Engdahl (1968) and Adams (1972) have observed that tunnelling energy is significant, since they find that $PmKP$ arrivals are often most noticeable at distances beyond the cut-off imposed by P waves bottoming at the core–mantle boundary. To obtain the total reflection coefficient for, say, $P4KP$, one need merely examine the product $T_{PK}R_{KK}{}^3T_{KP}$. This expression contains all the interaction of $P4KP$ with the core mantle interface. By examining the product

$$[T_{PK}g_{\omega p-1/2}^{(2)}(r_m)]\,R_{KK}{}^3[T_{KP}/g_{\omega p-1/2}^{(1)}(r_m)]$$

and observing that $|g_{\omega p-1/2}^{(2)}/g_{\omega p-1/2}^{(1)}| = 1$ for all real values of p, it also follows that the exponential decay between turning point and interface is automatically included in $T_{PK}R_{KK}{}^3T_{KP}$. (This decay originates from the $C^{(1)}+C^{(2)}$ of T_{PK}: see equation (22)). Values of the total $P4KP$ reflection coefficient are shown, as a function of ray parameter, in Fig. 7. Periods of 2 s and $\frac{1}{2}$ s are used, and also shown is the result of using plane wave coefficients. The latter method becomes inadequate for the longer period, for $p > 252$ s. Engdahl's (1968) and Adams' (1972) observations are satisfactorily explained by Fig. 7, since amplitudes for the two finite frequencies are highest at around 256s, beyond the core-grazing value of 254·6. At 2-s period, the reflection amplitude remains within a factor of 10 of its maximum for ray parameters

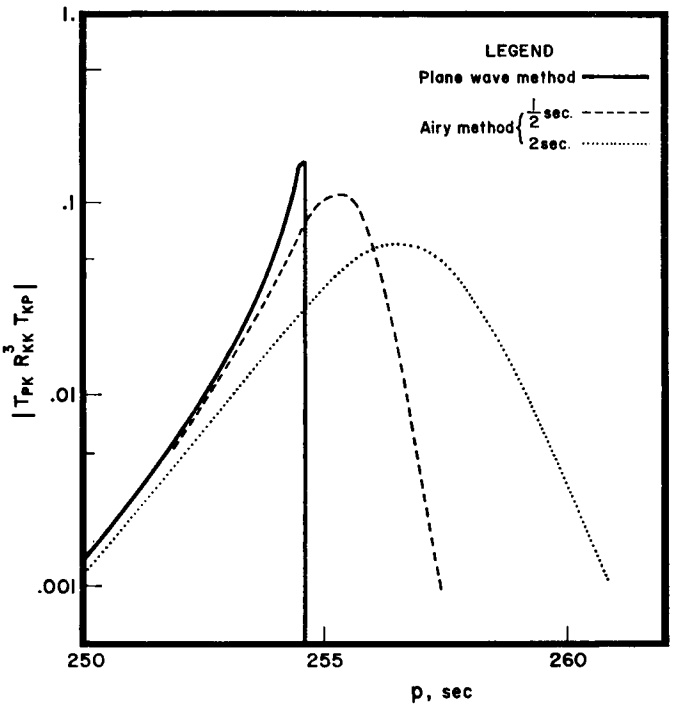

FIG. 7. Calculation of the tunnelling effect for the Earth model of Table 2. The total transmission coefficient for *P4KP* is shown as a function of ray parameter. Plane wave theory predicts a cutoff at $p = 254{\cdot}6$ s, due to the mantle ray just grazing the core. But the Airy method (formulae (23)) permits energy at finite frequencies to cross into the core, even from mantle ray paths which do not intersect the core.

up to 5 s beyond the core-grazing value. The frequency dependence of the reflection is remarkable, in that the shorter period has the greater amplitude for part of the tunnelling range. It is clear that attenuation in the outer core will be assigned too low a value (high Q) if plane wave coefficients are used.

The above results have been developed from a theory of high frequency waves. But, unfortunately, the asymptotic nature of WKBJ approximations makes it difficult to quantify any improved accuracy that results from using Airy functions where WKBJ theory breaks down. A test of the Airy function method can, however, be achieved, by using it in a canonical problem which has already been solved exactly. This is the problem of *P* waves near the shadow boundary of the Earth's core, in an Earth model with individually homogeneous mantle and core. Phinney & Cathles (1969) have obtained this solution in the form of equation (1), and have discussed the numerical integration. The exact integrand involves a *PcP* reflection coefficient in terms of Hankel functions, and resulting slowness and amplitudes of the potential for *P*+*PcP* waves are shown in Fig. 8(a) and (b). The Earth model used was just that of Phinney & Cathles, which has its shadow boundary at distance 113·5°. Fig. 8 shows also the result of doing the same integration (involving in the complex p-plane the path Γ of Fig. 5(d)), but approximating the mantle *P* wave by Airy functions of formulae (21). In this case both for the 1-s and 10-s periods, the Airy function method is clearly successful.

It is important for many wave propagation problems in the Earth to know the range of real ray parameters, or angles of incidence, within which plane wave reflection/transmission coefficients are inaccurate. No simple definitive answer can be given, but the range must crudely be given by those arguments of an Airy function for which

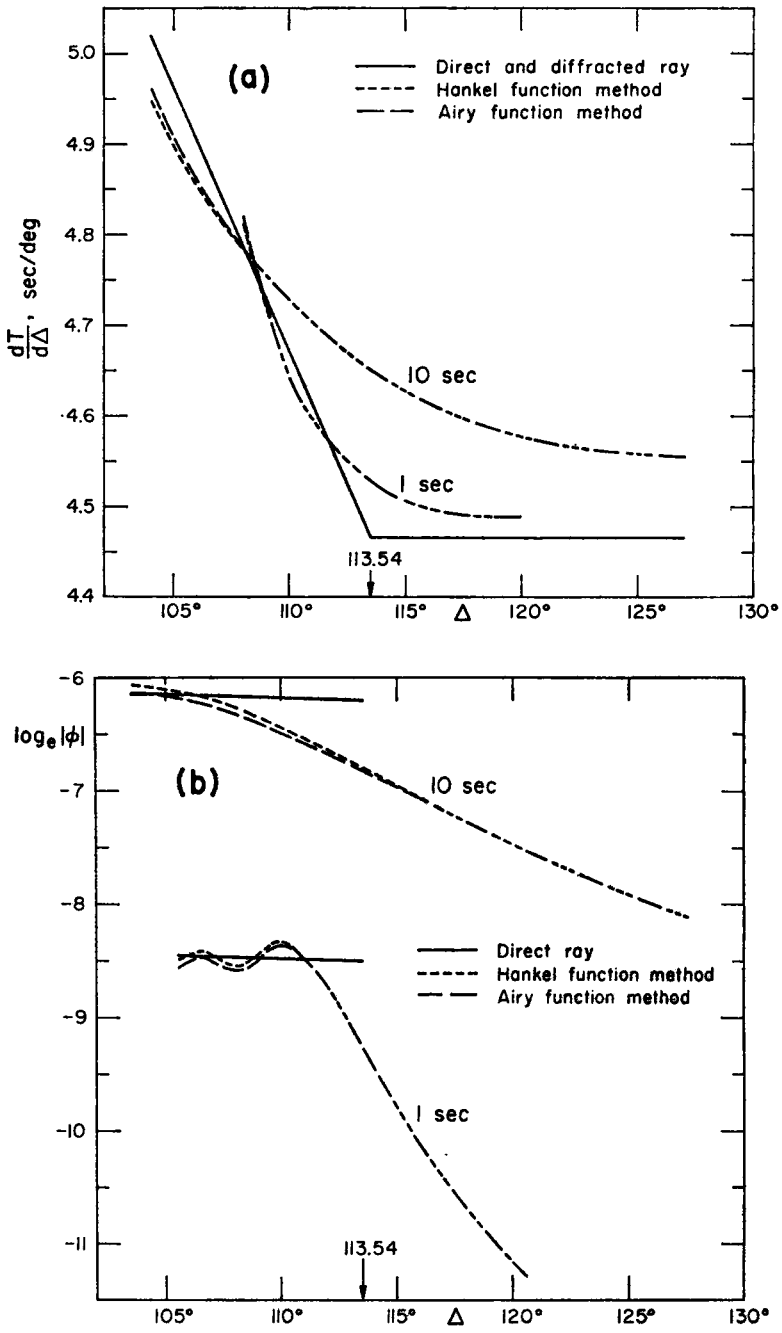

FIG. 8. *P*-wave potential slowness (a), and amplitude (b), due to a point source in a homogeneous mantle, computed for each of two periods by the exact (Hankel) and Airy function methods. Accuracy of the latter is verified.

WKBJ theory (for the Airy equation) is inadequate. The theory is in error by about 6 per cent for $Ai(z)$ when $z = 1$ or $z = -1$, and rapidly worsens as $z \to 0$. So one may expect, from the definition of the Airy function argument in (21), that plane wave coefficients will be inadequate for studying a boundary condition at radius r if the ray

parameter is in the range

$$\left| p - \frac{r}{\alpha(r)} \right| < \left(\frac{r}{2\alpha}\right)^{1/3} \left(\frac{1-b}{\omega}\right)^{2/3}.$$

As might be expected, this range is decreased for higher frequencies. It is also decreased for $b \sim 1$, implying a near critical velocity gradient. This also should be expected, for the standard Earth flattening transformation (Müller 1971) converts a spherical shell with gradient $(d\alpha/dr) = \alpha/r$ into a homogeneous plate, in which plane wave theory is exact.

Extension of basic methods

The emphasis above has been on calculating displacement components in the frequency domain in the form

$$u(\Delta_0, \omega) = \int_\Gamma \omega^{1/2} f(p, \Delta_0)\, e^{i\omega J(p, \Delta_0)}\, dp$$

for $\omega > 0$. But the dependence on frequency here is very simple, and if values of f and J are stored along Γ then the time domain solution may readily be obtained from

$$u(\Delta_0, t) = \frac{1}{\pi} \int_0^\infty \omega^{1/2} Re \left\{ \int_\Gamma f e^{i\omega J}\, dp\, e^{-i\omega t} \right\} d\omega. \tag{23}$$

Computation of theoretical seismograms via (23) may compare very favourably with the generalized Cagniard method for a spherically symmetric medium (Gilbert & Helmberger 1972). Both (23) and the Cagniard procedure would require Fourier integration (or convolution) for practical sources and instrument responses, so comparison of the methods must be between an integration over p, and calculation of a Cagniard path. Both paths are in the complex ray parameter plane, and both are required (in their different contexts) to be steepest descents paths (although Γ need only approximately be so). But in any given problem, the paths are completely different. The Cagniard path, for our analysis of the Fourier transform, would be exactly a path of stationary phase.

The principal merits of (23) are then: (i) that f and J are easily modified for different distances Δ_0, Γ remaining fixed, whereas the Cagniard path requires recalculation for each distance; (ii) that the method (23) will work for ray paths having a turning point, and the Cagniard method (as presently developed) apparently will not; (iii) that our method may be modified (by formulae (21), (22)) to study problems for which plane wave reflection/transmission coefficients are inadequate; and (iv) that (23) is not significantly complicated by allowing each velocity profile (α, β) to have an imaginary part, thus quantifying the effect of attenuation.

Conclusions

Short-period body waves in the Earth display a variety of properties (caustics, diffraction, tunnelling) which appear to require a full wave theory for their evaluation. But this evaluation is often accurately given by expressing wave solutions as an integration over complex ray parameter, the integrand being adequately given by WKBJ theory. (See equations (16) and (14)). The advantages lie in straightforward and rapid numerical computation, and in insight into wave properties, which are often predicted by inspection of features in the complex ray parameter plane.

Amplitudes and $dT/d\Delta$, calculated at finite frequencies near the caustic in *PKKP*, are found to be controlled by properties of the earlier travel-time branch. But for

PmKP ($m > 3$), the larger amplitudes are associated with the later travel-time branch, and are in fact largest for energy tunnelling into and out of the core from a mantle *P* wave ray with turning point somewhat above the core–mantle boundary.

Acknowledgments

I appreciate many helpful discussions with Dr C. H. Chapman. The original manuscript was improved by the critical reviews of Drs L. E. Alsop, J. E. Nafe and L. R. Sykes. This research was supported by the National Science Foundation under grant GA 34109.

References

Abramowitz, M. & Stegun, I. A., 1964. Handbook of mathematical functions, *U.S. Natl. Bur. Stan.*

Adams, R. D., 1972. Multiple inner core reflections of a Novaya Zemlya explosion, *Bull. seism. Soc. Am.*, **62**, 1063–1071.

Bolt, B. A. & Qamar, A., 1972. Observations of pseudo-aftershocks from underground nuclear explosions, *Phys. Earth planet. Int.*, **5**, 400–402.

Bullen, K. E., 1963. *Introduction to the theory of seismology*, third edition, Cambridge University Press.

Coddington, E. A. & Levinson, N., 1955. *Theory of ordinary differential equations*, McGraw-Hill Book Co.

Chapman, C. H., 1969. *Seismic wave diffraction theory*, Ph.D. thesis, University of Cambridge.

Chapman, C. H., 1973. The Earth flattening approximation in body wave theory, *Geophys. J. R. astr. Soc.*, **35**, 55–70.

Chapman, C. H. & Phinney, R. A., 1970. Diffraction of *P* waves by the core and an inhomogeneous mantle, *Geophys. J. R. astr. Soc.*, **21**, 185–205.

Chapman, C. H. & Phinney, R. A., 1972. Diffracted seismic signals and their numerical solution, in *Methods in Computational Physics*, **12**, 165–230, Academic Press.

Chester, C., Friedman, B. & Ursell, F., 1957. An extension of the method of steepest descent, *Proc. Camb. phil. Soc.*, **54**, 599–611.

Engdahl, E. R., 1968. Seismic waves within Earth's outer core: multiple reflection, *Science*, **161**, 263–264.

Friedman, B., 1951. Propagation in a non-homogeneous atmosphere, *Communs pure appl. Math.*, **4**, 317–350.

Gilbert, F. & Helmberger, D. V., 1972. Generalized ray theory for a layered sphere, *Geophys. J. R. astr. Soc.*, **27**, 57–80.

Haskell, N. A., 1962. Crustal reflection of plane *P* and *SV* waves, *Bull. seism. Soc. Am.*, **67**, 4751–4767.

Helmberger, D. V., 1968. The crust–mantle transition in the Bering Sea, *Bull. seism. Soc. Am.*, **58**, 179–214.

Helmberger, D. V. & Wiggins, R. A., 1971. Upper mantle structure of Midwestern United States, *J. geophys. Res.*, **76**, 3229–3245.

Jeffreys, H., 1939. The times of the core waves, *Mon. Not. R. astr. Soc., Geophys. Suppl.*, **4**, 548–561.

Jeffreys, H., 1962. *The Earth*, fourth edition, Cambridge University Press.

Julian, B. R. & Anderson, D. L., 1968. Travel times, apparent velocities, and amplitudes of body waves, *Bull. seism. Soc. Am.*, **58**, 339–366.

Morse, P. M. & Feshbach, H., 1953. *Methods of theoretical physics*, Vol. II, McGraw-Hill Book Co.

Müller, G., 1971. Approximate treatment of elastic body waves in media with spherical symmetry, *Geophys. J. R. astr. Soc.*, **23**, 435–449.

Nussenzveig, H. M., 1965. High-frequency scattering by an impenetrable sphere, *Ann. Phys. (N.Y.)*, **34**, 23–95.
Nussenzveig, H. M., 1969a. High-frequency scattering by a transparent sphere. I. Direct reflection and transmission, *J. math. Phys.*, **10**, 82–124.
Nussenzveig, H. M., 1969b. High-frequency scattering by a transparent sphere. II. Theory of the rainbow and the glory, *J. math. Phys.*, **10**, 125–176.
Phinney, R. A. & Alexander, S. S., 1966. *P* wave diffraction theory and the structure of the core–mantle boundary, *J. geophys. Res.*, **71**, 5959–5975.
Phinney, R. A. & Cathles, L. M., 1969. Diffraction of P by the core: a study of long-period amplitudes near the edge of the shadow, *J. geophys. Res.*, **74**, 1556–1574.
Rayleigh, Lord, 1912. On the propagation of waves through a stratified medium, with special reference to the question of reflection, *Proc. R. Soc. Lond., Ser. A*, **86**, 207–226.
Richards, P. G., 1970. *A contribution to the theory of high frequency elastic waves, with applications to the shadow boundary of the Earth's core*, Ph.D. thesis, California Institute of Technology.
Richards, P. G., 1971a. Potentials for elastic displacement in spherically symmetric media, *J. acoust. Soc. Am.*, **50**, 188–197.
Richards, P. G., 1971b. An elasticity theorem for heterogeneous media, with an example of body wave dispersion in the Earth, *Geophys. J. R. astr. Soc.*, **22**, 453–472.
Richards, P. G., 1973. *Bull. seism. Soc. Am.*, submitted.
Scholte, J. G. J., 1956. On seismic waves in a spherical Earth, *Koninkl. Med. meteorol. Inst. Publ.*, **65**, 1–55.
Seckler, B. D. & Keller, J. B., 1959. Asymptotic theory of diffraction in inhomogeneous media, *J. acoust. Soc. Am.*, **31**, 206–216.
Werth, G. C. & Herbst, R. F., 1963. Comparison of amplitudes of seismic waves from nuclear explosions in four mediums, *J. geophys. Res.*, **68**, 1463–1475.

Appendix

The partial wave expansion (6) is here manipulated into a form more suitable for computation. We use the Watson transform

$$\sum_{n=0}^{\infty} f(n+\tfrac{1}{2}) = \tfrac{1}{2} \int_C f(\nu)\, e^{-i\nu\pi} \sec \nu\pi \, d\nu \qquad \text{(A1)}$$

where C is taken around the positive real ν-axis, and is shown in Fig. A1(a). The two cases to be considered are as follows.

Case A. Source below receiver, ray departing upwards.

This configuration is shown in Fig. 1(a), and note that there is no turning point along the ray path.

Writing (6) as

$$\phi = L_s \sum_{n=0}^{\infty} (2n+1)\, g_n^{(1)}(r)\, f_n(r_s)\, e^{2in\pi}\, P_n(\cos\Delta)$$

(note the introduction of $e^{2in\pi} = 1$, required below for convergence in part of the upper half of the complex order plane), we may use (A1) to find

$$\phi = -L_s \int_C \nu g_{\nu-1/2}^{(1)}(r)\, f_{\nu-1/2}(r_s)\, P_{\nu-1/2}(\cos\Delta)\, e^{i\nu\pi} \sec \nu\pi \, d\nu.$$

The work of Nussenzveig (1965, equations (2.20) and (2.35)) shows that C may be deformed across the first quadrant, and parts of the second and fourth, into path C_0

(Fig. A1(b)), which is symmetric about the origin. Writing

$$P_{\nu-1/2}(\cos\Delta)\sec\nu\pi = -i[Q_{\nu-1/2}^{(2)}(\cos\Delta) - Q_{-\nu-1/2}^{(2)}(\cos\Delta)]\operatorname{cosec}\nu\pi,$$

the integral along C_0 may be split into two terms. Replacing ν by $-\nu$ in the integral containing $Q_{-\nu-1/2}^{(2)}$, and using

$$f_{-\nu-1/2}(r_s) = f_{\nu-1/2}(r_s)\,e^{i\nu\pi} - i\sin\nu\pi g_{\nu-1/2}^{(2)}(r_s),$$

it is seen that there is a cancellation of parts of the two terms, and

$$\phi = -L_s\int_{C_0}\nu g_{\nu-1/2}^{(1)}(r)\,g_{\nu-1/2}^{(2)}(r_s)\,Q_{\nu-1/2}^{(2)}(\cos\Delta)\,d\nu.$$

The Watson poles have at this stage been transferred to the negative real ν-axis ($Q_n^{(2)}$ having poles at the negative integers), and, reversing the direction of C_0, we find

$$\phi = L_s\int_{C_1}\nu g_{\nu-1/2}^{(1)}(r)\,g_{\nu-1/2}^{(2)}(r_s)\,Q_{\nu-1/2}^{(2)}(\cos\Delta)\,d\nu \qquad \text{(A2)}$$

where C_1 is shown in Fig. A1(c).

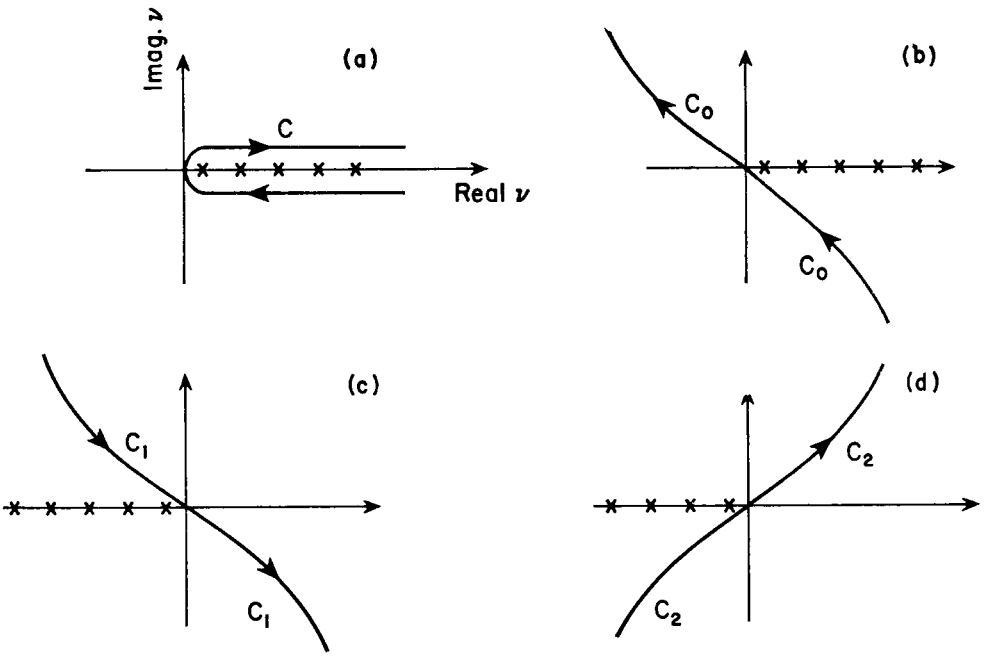

FIG. A1. (a) Path for Watson transformation. Poles occur at $\nu = n+\frac{1}{2}$, $n = 0, 1, 2, 3, \ldots$. (b) Deformation of C, for direct ray with no turning point. (c) As for C_0, after $Q_{-\nu-1/2}^{(2)}$ integration is reflected in the origin, and C_0 direction is reversed. (d) Deformation of C, for direct ray with turning point, and after $Q_{-\nu-1/2}^{(2)}$ integration is reflected in the origin.

Case B. Source below receiver, ray departing downwards.

This configuration is shown in Fig. 2(a), and note that a turning point is now present.

Using $P_n(\cos\Delta) = e^{in\pi}P_n(-\cos\Delta)$, one sees from (6) that

$$\phi = L_s\sum_{n=0}^{\infty}(2n+1)\,g_n^{(1)}(r)f_n(r_s)\,e^{in\pi}P_n(-\cos\Delta),$$

and then from (A1) that

$$\phi = -iL_s \int_C \nu g_{\nu-1/2}^{(1)}(r) f_{\nu-1/2}(r_s) P_{\nu-1/2}(-\cos\Delta) \sec \nu\pi \, d\nu.$$

It follows from Nussenzveig (1965, equations (2.19) and (2.34)) that C may be deformed across the fourth quadrant, and parts of the first and third, into path C_2 (see Fig. A1(d)), which is symmetric about the origin. At this stage, the integrand has poles on the positive real ν-axis. Writing

$$P_{\nu-1/2}(-\cos\Delta) \sec \nu\pi = [-e^{-i\nu\pi} Q_{\nu-1/2}^{(2)}(\cos\Delta) + e^{i\nu\pi} Q_{-\nu-1/2}^{(2)}(\cos\Delta)] \operatorname{cosec} \nu\pi,$$

and using

$$f_{-\nu-1/2}(r_s) = f_{\nu-1/2}(r_s) e^{-i\nu\pi} + i \sin \nu\pi g_{\nu-1/2}^{(1)}(r_s),$$

it is seen that the method used for Case A again permits the poles to be shifted to the negative real ν-axis, and in fact there results

$$\phi = L_s \int_{C_2} \nu g_{\nu-1/2}^{(1)}(r) \, g_{\nu-1/2}^{(1)}(r_s) \, Q_{\nu-1/2}^{(2)}(\cos\Delta) \, d\nu. \tag{A3}$$

The formulae (A2) and (A3) display the two simplifying properties claimed for the (Watson) transformed solution. Namely, that only the expected one term (of four terms) is retained from the expansion (6), and that it is integrated over a complex path with no prior scalar multiplication.